Advances in Applied Mathematics and Mechanics
Adv. Appl. Math. Mech., Vol. **8**, No. 1, pp. 52-66

DOI: 10.4208/aamm.2014.m462
February 2016

# Unsteady MHD Non-Darcian Flow Over a Vertical Stretching Plate Embedded in a Porous Medium with Thermal Non-Equilibrium Model

D. Prakash[1], M. Muthtamilselvan[1,*] and Xiao-Dong Niu[2]

[1] *Department of Applied Mathematics, Bharathiar University, Coimbatore-641 046, India*
[2] *Department of Mechatronics Engineering, Shantou University, Shantou 515063, China*

Received 10 January 2014; Accepted (in revised version) 28 November 2014

**Abstract.** An analysis is performed to study the influence of local thermal non-equilibrium (LTNE) on unsteady MHD laminar boundary layer flow of viscous, incompressible fluid over a vertical stretching plate embedded in a sparsely packed porous medium in the presence of heat generation/absorption. The flow in the porous medium is governed by Brinkman-Forchheimer extended Darcy model. A uniform heat source or sink is presented in the solid phase. By applying similarity analysis, the governing partial differential equations are transformed into a set of time dependent non-linear coupled ordinary differential equations and they are solved numerically by Runge-Kutta Fehlberg method along with shooting technique. The obtained results are displayed graphically to illustrate the influence of different physical parameters on the velocity, temperature profile and heat transfer rate for both fluid and solid phases. Moreover, the numerical results obtained in this study are compared with the existing literature in the case of LTE and found that they are in good agreement.

**AMS subject classifications**: 76D10, 76S05, 76W05

**Key words**: MHD, Brinkman-Forchheimer model, heat generation, local thermal non-equilibrium (LTNE).

## 1 Introduction

The transport in porous media is a process that finds application in a broad spectrum of disciplines ranging from chemical engineering to geophysics. For instance, applications

*Corresponding author.
*Email:* muthtamil1@yahoo.co.in (M. Muthtamilselvan), dsprakash86@gmail.com (D. Prakash)

 

of the porous media includes, heat exchangers, geothermal systems, building thermal insulation, nuclear waste disposal, thermal energy storage cooling of nuclear reactors during emergency shutdown etc. to name just few. To be more specific, it may be pointed out that many metallurgical processes involve the cooling of continuous strips or filaments by drawing them through a quiescent fluid and that in the process of drawing, these strips are sometimes stretched. For example in the case of drawing, annealing and tinning of copper wires, the properties of the final product depend to a great extent on the rate of cooling. By drawing such strips in a porous medium [1] and by applying magnetic field, the rate of cooling can be controlled and a final product of desired characteristics can be achieved. Reviews of the huge volume of information on this subject is amply documented in the recent books by Nield and Bejan [2], Vafai [3] and Ingham and Pop [4].

Most of the earlier studies on flow through porous media have been employed with the Darcy model. But in many applications in engineering disciplines involve high permeability porous media. In such situation, Darcy equation fails to give satisfactory results. Therefore, use of non-Darcy models, which takes care of boundary and/or inertia effects, is of fundamental and practical interest to obtain accurate results for high permeability porous media. The inertial and the solid boundary effects on momentum and energy transport have been discussed through constant-porosity media [5] and through non-uniform porosity media [6]. These investigations provided an insight on the applicability of the customarily employed Darcy's law. Due to the importance of non-Darcian effects in the emerging industrial and engineering applications, several researchers [7–11] have analyzed the boundary layer flow characteristics by assuming non-Darcian model.

Most of the analytical and numerical studies of flow and heat transfer in porous media assume the condition of local thermal equilibrium (LTE) between the solid and the fluid materials, i.e., it is assumed that the temperature difference at any location between the two phases is absent. This assumption is satisfactory for small-pore media such as geothermal reservoirs and fibrous insulations and small temperature difference between the phases. But for many practical applications, involving high-speed flows or large temperature difference between the fluid and solid phases, the assumption of local thermal equilibrium is inadequate and it is important to take account of the thermal non-equilibrium effects. Furthermore, when the length scale of the representative control volume is the same order of the length of the system, then the thermal equilibrium model prediction may be unacceptable [12]. Due to applications of porous media theory in drying/freezing of foods [13, 14] and othermundane materials and applications in everyday technology such as microwave heating [15], rapid heat transfer from computer chips via use of porous metal foams [16, 17] and their use in heat pipes, it is believed that the local thermal non-equilibrium (LTNE) theory will play a major role in future developments.

Reasonably a good number of papers have been focused on impact of LTNE state on convective flow in connection with horizontal cylinder [18], cavity [19, 20] and channel [21, 22]. In recent years, the effect of local thermal non-equilibrium on natural convection over a vertical plate has been studied by several authors. Much of this study has

been reviewed in recent book by Ingham and Pop [4]. Rees and Pop [23] studied the effect of local thermal equilibrium on the free convective boundary layer flow in the porous vertical plate. They found that the thermal equilibrium is achieved by increasing the distance from the leading edge. Mixed convection in a vertical porous layer under LTNE assumption has been investigated by Saeid [24]. It is reported that the total average Nusselt number depends strongly on the thermal conductivity ratio parameter and slightly on the heat transfer co-efficient parameter i.e., increasing the thermal conductivity ratio leads to increase in the total average Nusselt number. Nouri-Borujerdi et al. [25] derived the simple conditions to guarantee local thermal equilibrium for conduction in porous channels with heat source. Thermal non-equilibrium heat transfer in the stagnant porous medium with variable porosity is analyzed by Nazari and Kowsari [26], where the heat generation takes place within the solid phase. Darcy's flow in a horizontal porous layer with impermeable boundaries is studied by Barletta and Celli [27] in the case of LTNE model. The viscous dissipation effect is taken into account and the local thermal non-equilibrium model for the energy balance is adopted. Very recently, Muthtamilselvan et al. [28] have analyzed the influence of thermal non-equilibrium on transient hydromagnetic boundary layer flow of nanofluid past a vertical stretching surface.

Based on the assumption of sinusoidal temperature oscillation on the plate (Saeid and Mohamad [29]), we have assumed that the plate temperature linearly varies with time and distance. The present study is to investigate the magnetic field and local thermal non-equilibrium on unsteady boundary layer flow over a stretching vertical plate embedded in a porous medium with heat generation/absorption. By using the similarity approach, the transport equations are transformed into non-linear ODE and they are solved numerically.

## 2 Mathematical formulation

Consider an unsteady two-dimensional laminar boundary layer flow over a continuous moving stretching plate in a viscous incompressible electrically conducting fluid saturated porous medium. A uniform magnetic field $B=[0,B_0(x)]$ is applied in the direction perpendicular to the stretching surface and varies in strength as a function of $x$. Since the transverse applied magnetic field and magnetic Reynolds number are assumed to be small, the induced magnetic field can be neglected. The $x$-axis is taken along the stretching plate in the direction of the motion and the $y$-axis is perpendicular to the plate in the outward direction towards the fluid of ambient temperature $T_\infty$ (see Fig. 1).

We assume that for time $t<0$ the fluid and heat flows are steady. The unsteady fluid and heat flows start at $t=0$, the plate is being stretched with the velocity $U_w(x,t)=ax/1-ct$ along the $x$-axis, where $a$ (stretching rate) and $c$ are positive constants having dimension $t^{-1}$ (with $ct<1$, $c\geq 0$). In case of polymer extrusion, the material properties of the extruded sheet may vary with time. Here, the stretching sheet is subjected to such amount of tension which does not alter the structure of the porous material. The surface

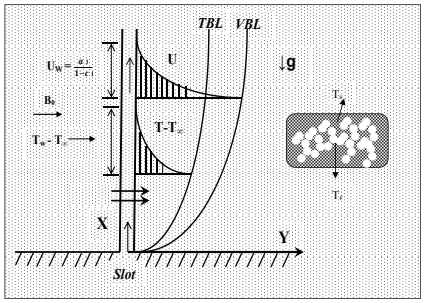


Figure 1: Physical configuration and coordinate system.

temperature of the plate varies with the distance $x$ from the slot and time $t$ in the form

$$T_w(x,t) = T_\infty + \frac{bx}{1-ct}, \tag{2.1}$$

where $b$ is a constant and has a dimension temperature/length, with $b>0$ and $b<0$ corresponding to the assisting and opposing flows, respectively, and $b=0$ is for the forced convection limit (absence of buoyancy force). The Brinkman-Forchheimer extended Darcy model is used as the momentum equation

$$\frac{\partial u}{\partial x} + \frac{\partial v}{\partial y} = 0, \tag{2.2a}$$

$$\frac{\partial u}{\partial t} + u\frac{\partial u}{\partial x} + v\frac{\partial u}{\partial y} = -\frac{\mu\epsilon}{\rho k}u + \frac{\bar{\mu}}{\rho}\frac{\partial^2 u}{\partial y^2} - \frac{C_b\epsilon^2}{\sqrt{k}}u^2 + g\beta(T_f - T_\infty) - \frac{\sigma_m B_0^2(x)}{\rho}u, \tag{2.2b}$$

$$\epsilon(\rho c_p)_f\left(\frac{\partial T_f}{\partial t} + u\frac{\partial T_f}{\partial x} + v\frac{\partial T_f}{\partial y}\right) = \epsilon k_f\left(\frac{\partial^2 T_f}{\partial y^2}\right) + h(T_s - T_f), \tag{2.2c}$$

$$(1-\epsilon)(\rho c_p)_s\frac{\partial T_s}{\partial t} = (1-\epsilon)\left(k_s\frac{\partial^2 T_s}{\partial y^2}\right) - h(T_s - T_f) + (1-\epsilon)q''', \tag{2.2d}$$

and the initial, boundary conditions are

$$u = U_w(x,t), \quad v = 0, \quad T_f = T_w(x,t), \quad T_s = T_w(x,t) \quad \text{at } y = 0, \tag{2.3a}$$

$$u \to 0, \quad T_f \to T_\infty, \quad T_s \to T_\infty \quad \text{as } y \to \infty, \tag{2.3b}$$

where $u$ and $v$ are the velocity components along $x$ and $y$ directions, respectively. $\rho$ is the fluid density, $\bar{\mu}$ is the effective viscosity of the fluid, $\mu$ is the fluid viscosity, $k$ is the permeability, $\epsilon$ is the porosity of the saturated porous medium, $C_b$ is the empirical constant of the second-order resistance term due to inertia effect, $g$ is the acceleration due to gravity, $\beta$ is the coefficient of thermal expansion, $c_p$ is the specific heat at constant pressure, $\sigma_m$ is the magnetic permeability of the fluid and $B_0(x)$ is the applied magnetic field, $q'''$ is the volumetric heat generation in the solid phase. $T_f$, $T_s$ and $k_f$, $k_s$ are the temperature and

thermal conductivity of the fluid and solid, $h$ is the interstitial heat transfer coefficient between the solid and fluid phases.

The inter-phase heat transfer coefficient $h$ depends on the nature of the porous matrix and the saturating fluid and the value of this coefficient has been the subject of intense experimental interest. Large values of $h$ correspond to a rapid transfer of heat between the phases (LTE) and small values of $h$ gives rise to relatively strong thermal non-equilibrium effects (Malashetty et al. [30]).

We now introduce a stream function $\psi(x,y,t)$, which is defined by

$$u=\frac{\partial\psi}{\partial y},\quad v=-\frac{\partial\psi}{\partial x}. \tag{2.4}$$

The mathematical analysis of the problem is simplified by introducing the dimensionless functions $f$, $\theta_f$, $\theta_s$ in terms of the similarity variable $\eta$ (see Ishak et al. [31], Muthtamilselvan and Prakash [32]) as

$$\eta=y\sqrt{\frac{U_w}{\nu x}},\quad \psi=\sqrt{\nu x U_w}f(\eta),\quad \theta_f=\frac{T_f-T_\infty}{T_w-T_\infty},\quad \theta_s=\frac{T_s-T_\infty}{T_w-T_\infty}. \tag{2.5}$$

Substituting Eqs. (2.4)-(2.5) into the governing equations (2.2a)-(2.2d), we get the following transformed equations:

$$f'''+ff''-f'^2-A\left(f'+\frac{1}{2}\eta f''\right)+\lambda\theta_f-\frac{\alpha^*}{\sigma Re}f'-\beta^*f'^2-Mf'=0, \tag{2.6a}$$

$$\frac{1}{Pr}\theta_f''-A\left(\frac{\eta\theta_f'}{2}+\theta_f\right)-f'\theta_f+f\theta_f'+H(\theta_s-\theta_f)=0, \tag{2.6b}$$

$$\frac{1}{Pr}\theta_s''-A\left(\frac{\eta\theta_s'}{2}+\theta_s\right)-H\gamma\epsilon_s(\theta_s-\theta_f)+Q\theta_s=0, \tag{2.6c}$$

and the boundary conditions

$$f(0)=0,\quad f'(0)=1,\quad \theta_f(0)=1,\quad \theta_s(0)=1, \tag{2.7a}$$

$$f'(\infty)=0,\quad \theta_f(\infty)=0,\quad \theta_s(\infty)=0, \tag{2.7b}$$

where prime denotes the differentiation with respect to $\eta$, $A=c/a$ is the unsteady parameter, $\lambda=Gr/Re_x^2$ is the buoyancy parameter, $M=\sigma_m B_0^2 x/\rho U_w$ is the local magnetic parameter, $\beta^*=C_b\epsilon^2 x/\sqrt{k}$ is the local inertial parameter, $Pr=\nu/\alpha$ is the Prandtl number and $Q=q'''x/(\rho c_p)_s U_w$ is the dimensionless heat generation/absorption parameter, where $\nu=\bar{\mu}/\rho$, $\alpha=k/\rho c_p$, $Gr=g\beta(T_w-T_\infty)x^3/\nu^2$ is the local Grashof number, $Re_x=U_w x/\nu$ is the local Reynolds number, $\alpha^*=\mu/\bar{\mu}$ is the ratio of viscosities and $\sigma=k/x^2\epsilon$ is the local permeability parameter.

The non-dimensional parameters, $H$, $\gamma$ and $\epsilon_s$ are the non-dimensional inter-phase heat transfer parameter, the porosity modified conductivity ratio and the fluid/solid

modified thermal diffusivity ratio:

$$H=\frac{hx\alpha_f}{U_w\epsilon k_f},\quad \gamma=\frac{\epsilon k_f}{(1-\epsilon)k_s},\quad \epsilon_s=\frac{\alpha_s}{\alpha_f}. \tag{2.8}$$

The important characteristics of the flow are the skin-friction co-efficient $C_f$ and the local Nusselt numbers for fluid and solid phases $Nu_f$ and $Nu_s$, which are defined as

$$C_f=\frac{\tau_w}{\rho U_w^2/2},\quad Nu_f=\frac{x(q_w)_f}{k_f(T_w-T_\infty)},\quad Nu_s=\frac{x(q_w)_s}{k_s(T_w-T_\infty)}, \tag{2.9}$$

where the wall shear stress $\tau_w$, the surface heat fluxes for fluid and solid are given by

$$\tau_w=\mu\Big(\frac{\partial u}{\partial y}\Big)_{y=0},\quad (q_w)_f=-k_f\Big(\frac{\partial T}{\partial y}\Big)_{y=0},\quad (q_w)_s=-k_s\Big(\frac{\partial T}{\partial y}\Big)_{y=0}. \tag{2.10}$$

Substituting Eq. (2.10) in (2.9), we get

$$\frac{1}{2}C_f\sqrt{Re_x}=f''(0),\quad Nu_f/\sqrt{Re_x}=-\theta_f'(0),\quad Nu_s/\sqrt{Re_x}=-\theta_s'(0), \tag{2.11}$$

where $Re_x=U_wx/\nu$ is the local Reynolds number based on the surface velocity.

## 3 Numerical procedure

The coupled system of Eqs. (2.6a)-(2.6c) is highly non-linear. Most of the physical systems are inherently non-linear in nature and are of great interest to physicists, engineers and mathematicians. Problems involving non-linear ordinary differential equations are difficult to solve exactly. So, the governing equations together with the boundary conditions have to be solved numerically.

The system of equations subject to the boundary conditions (2.7) are solved numerically by Runge-Kutta-Fehlberg method along with shooting technique using MATLAB. Its accuracy and robustness has been repeatedly confirmed in various heat transfer papers. The asymptotic boundary conditions given by Eq. (2.7) are replaced by using a value of 15 for the similarity variable $\eta_{\max}$ as follows:

$$\eta_{\max}=15,\quad f'(15)=0,\quad \theta_s(15)=0,\quad \theta_f(15)=0. \tag{3.1}$$

The choice of $\eta_{\max}=15$ ensured that all numerical solutions approached the asymptotic values correctly. Pantokratoras [33] noticed that the erroneous result is found by many researchers in the field of convective heat and mass transfer because of taking small far-field asymptotic value of $\eta_{\max}$ during their numerical computation.

The present method is verified by comparing the results with previously published data [34,35] for the case of thermal equilibrium model. The data for comparison with the thermal equilibrium model is obtained by setting the variables $H=10^6$, $\gamma=10^2$ and $\epsilon_s=10^2$ at which the thermal equilibrium condition is recovered. Table 1 shows the comparative results.

Table 1: Comparison of results of the wall temperature gradient with Ishak et al. [34] and Vajravelu et al. [35] for $(M=\beta^*=A=0,\ \alpha^*/\sigma Re_x=0,\ Q=0)$.

| $\lambda$ | $Pr$ | Ishak et al. $\theta'(0)$ | Vajravelu et al. $\theta'(0)$ | Present results | |
|---|---|---|---|---|---|
| | | | | $\theta'_s(0)$ | $\theta'_f(0)$ |
| 0 | 0.72 | 0.8086 | 0.808836 | 0.808570 | 0.808578 |
| | 1.0 | 1.0000 | 1.000000 | 0.999927 | 0.999937 |
| | 3.0 | 1.9237 | 1.923687 | 1.923556 | 1.923573 |
| | 10.0 | 3.7207 | 3.720788 | 3.720444 | 3.720475 |
| 1.0 | 1.0 | 1.0873 | 1.087206 | 1.087209 | 1.087219 |
| 2.0 | | 1.1429 | 1.142298 | 1.142271 | 1.142281 |
| 3.0 | | 1.1853 | 1.185197 | 1.185222 | 1.185232 |

# 4 Results and discussion

Here, we discuss the effect of magnetic, non-Darcy, heat generation/absorption parameters on the flow and heat transfer characteristics in the case of local thermal/non-thermal equilibrium between the fluid and solid-matrix phases. In all the results to be reported below, the Darcian and thermal equilibrium effects are characterized with the negligible inertial effect ($\beta^*$) and large values of interphase heat transfer co-efficient ($H$) and/or porosity modified conductivity ratio ($\gamma$) respectively. The default values of the parameters are considered as $M=1$, $\lambda=1$, $\alpha^*/\sigma Re_x=0.1$, $Pr=0.72$, $H=1$, $\gamma=1$, $\epsilon_s=1$, $Q=-0.5$ unless otherwise specified.

The influence of magnetic parameter $M$ on the velocity profile for both cases of Darcy and non-Darcy region is depicted in Fig. 2. It can be seen that with the fixed value of unsteady parameter, the effect of increasing of magnetic parameter is to decrease the velocity profile near the plate, which is due to the fact that the transverse magnetic field gives rise to a resistive-type of force called Lorentz force. This force has a tendency to slow down the motion of the fluid which results in reducing the velocity profile. This qualitative reduction is observed in both cases of Darcy and non-Darcy region. However, more reduction is attained by applying non-Darcy effects in the flow field, since the fluid inertia provides an additional pressure loss in the flow field. Moreover, with the fixed values of magnetic parameter, the effect of increasing values of unsteady parameter $A$ is to decrease the velocity profile and hence it reduces the momentum boundary layer thickness.

The effect of free convection parameter $\lambda$ on the velocity field is shown in Fig. 3. In the case of steady state, an increase in the buoyancy parameter is to increase the velocity distribution and consequently increase it's boundary layer thickness. Also in the region of higher buoyancy parameter, a peak is observed near the stretching boundary, which exponentially decreases away from the stretching surface i.e., the free stream velocity near the surface is higher than that of the stretching surface velocity. Physically, it means that the free convection currents are carried away from the stretching surface to the free stream and as the free stream is in the upward direction, the free convection currents

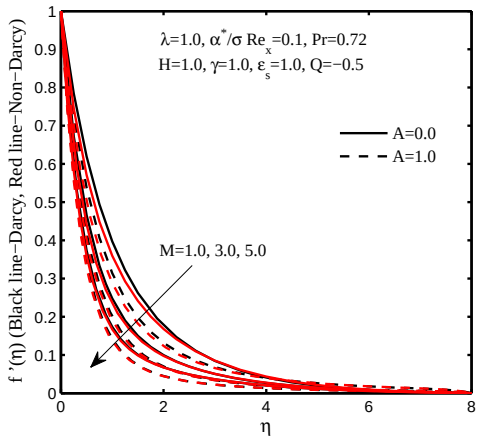


Figure 2: Velocity profile for different values of magnetic parameter and unsteady parameter.

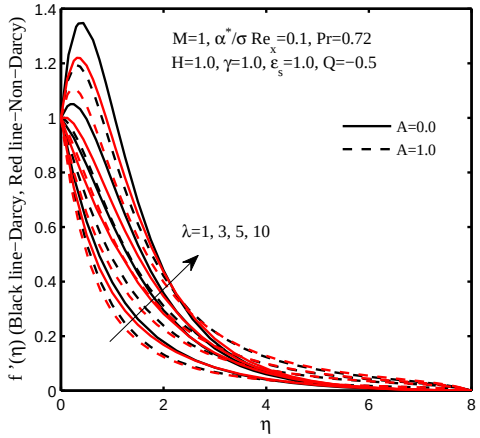


Figure 3: Velocity profile for different values of buoyancy parameter and unsteady parameter.

induce the fluid velocity to increase more. It is worth mentioning that the presence of non-Darcy effect is to decrease the fluid velocity near the stretching boundary because of higher retardation to the fluid. Furthermore, an increase in the dimensionless time parameter is to decrease the velocity profile, which causes reduction in the boundary layer thickness.

Figs. 4-7 are plotted to study the influence of heat generation/absorption parameters on the LTNE and LTE temperature profiles in the case of Darcy and non-Darcy flow respectively. It is found that the temperature distribution of solid and fluid phases increases with increase in the heat source parameter ($Q>0$), whereas decreases with increase in the heat sink ($Q<0$) parameter as expected. It is noted that with the assumption of LTNE between the phases, the higher heat generation parameter ($Q>0.5$) creates a distinctive type of peak near the stretching surface, which meant that the temperature profile for the

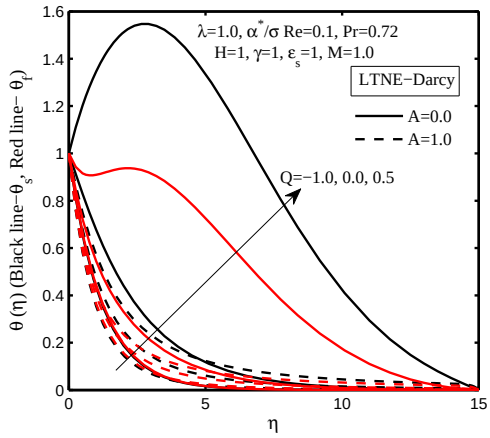


Figure 4: Temperature profile for different values of heat source/sink parameters in the case of Darcian flow (LTNE).

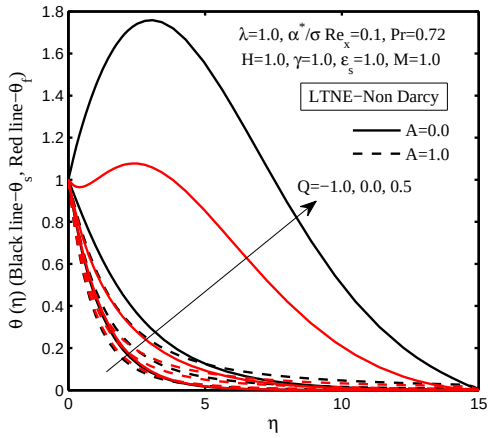


Figure 5: Temperature profile for different values of heat source/sink parameters in the case of Non-Darcian flow (LTNE).

fluid and solid-matrix phases near the stretching sheet is higher than that of the temperature of the stretching sheet and consequently the heat is expected to transfer from the free stream to the stretching surface. This phenomenon is signalled by the occurrence of the Sparrow-Gregg-type "hills". But, this behaviour is controlled/reversed with the inclusion of unsteady or heat sink parameters, i.e., the heat is transferred from the stretching surface to the free stream (see Figs. 4-5). However, such a type of hill is not observed by the assumption of thermal equilibrium between the fluid and solid-matrix phases (see Figs. 6-7).

Comparing the various Darcy/non-Darcy flow field on the temperature profile, one can easily realize that the temperature distribution for fluid and solid-matrix phases is

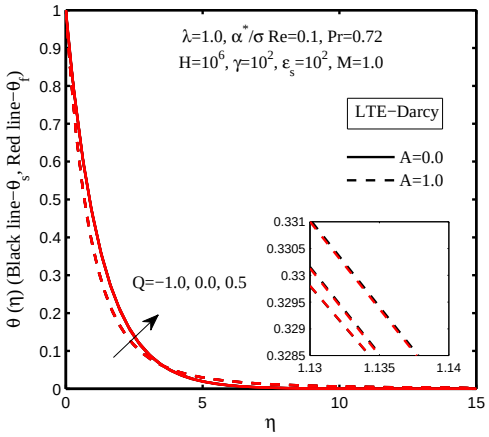


Figure 6: Temperature profile for different values of heat source/sink parameters in the case of Darcian flow (LTE).

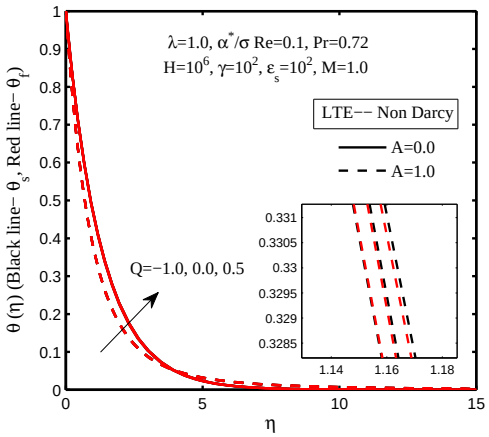


Figure 7: Temperature profile for different values of heat source/sink parameters in the case of Non-Darcian flow (LTE).

increased with the inclusion of non-Darcy effect (see Figs. 4-7). This is due to the fact that the flow boundary/inertia force retards the momentum transport which results in generation of form-drag and thereby increases the temperature.

Figs. 8-9 elucidate that the variation of local heat transfer rate for solid and fluid phases with different values of pertinent parameters such as $Pr$, $A$, $H$ and $\gamma$. It is noted from the Fig. 8 that in the view of lower values of $H$ or $\gamma$, the heat transfer rate of fluid phase is always higher than that of solid-matrix phase in all the cases $Pr$ and $A$. Furthermore, an increase in the interphase heat transfer co-efficient $H$ leads to increase the heat transfer rate for solid phase whereas, decrease the fluid heat transfer rate. However, an increase in $\gamma$ is to increase the heat transfer rate for both fluid and solid phases. In the case of large values of $H$ or $\gamma$, the temperature difference between the fluid and solid phases is

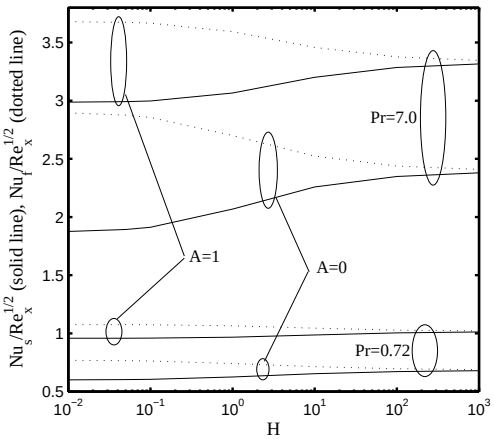


Figure 8: Nusselt number variation for solid and fluid with Prandtl number, unsteady parameter and inter-phase heat transfer coefficient.

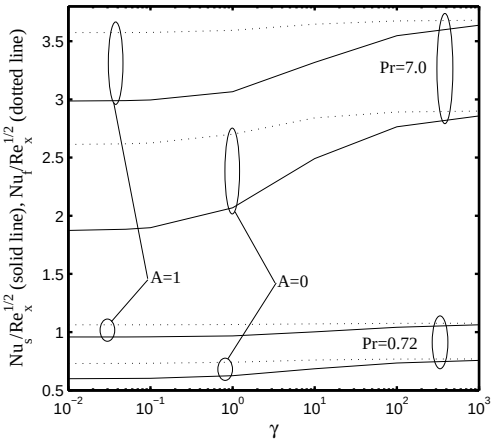


Figure 9: Nusselt number variation for solid and fluid with Prandtl number, unsteady parameter and modified thermal conductivity ratio.

negligible, i.e., local thermal equilibrium between the phases is attained. Moreover, it is noted that there may be some early departure from local thermal equilibrium is obtained for large values of Prandtl number, whereas the dimensionless time parameter controls it.

Figs. 10-11 demonstrate that the variation of heat transfer rate for solid and fluid phases with different values of interphase heat transfer co-efficient and thermal conductivity ratio and with different heat generation/absorption parameters. In the process of rapid cooling ($Q<0$), an increase in the interphase heat transfer co-efficient $H$ lead to decrease the solid heat transfer rate, whereas increase the fluid heat transfer rate up to the level of solid-matrix temperature. But the reverse trend has been observed during the process of rapid heating ($Q>0$). Further, we noticed that the fluid and solid-matrix phases may

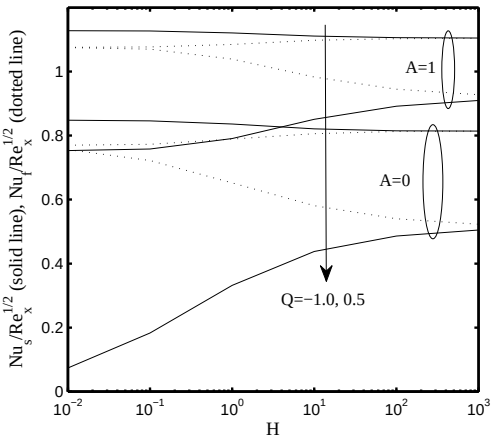


Figure 10: Nusselt number variation for solid and fluid with Heat generation/absorption, unsteady parameter and inter-phase heat transfer coefficient.

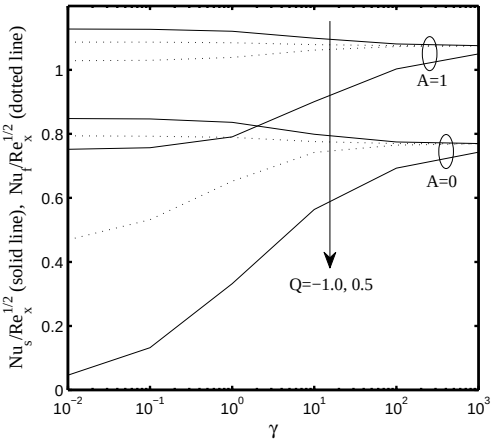


Figure 11: Nusselt number variation for solid and fluid with Heat generation/absorption, unsteady parameter and modified thermal conductivity ratio.

lead to attain thermal equilibrium very quickly during the process of rapid cooling, compared to rapid heating. These results are observed in both cases of steady and unsteady situations.

When the heat is absorbed from the solid-matrix phase ($Q<0$), an increase in the porosity modified conductivity ratio ($\gamma$) is to decrease the heat transfer rate for both fluid and solid-matrix phases. Whereas, in the case of heat is generated ($Q>0$) to solid-matrix phase, the parameter $\gamma$ lead to increase the solid-fluid heat transfer rates, as expected. Also, we found that the unsteady parameter $A$ is to decrease the temperature difference between the fluid and solid phases for the case of generating/absorbing heat from the solid-matrix phase.

## 5 Conclusions

We have attempted to establish the condition of early departure from local thermal equilibrium for the problem of transient MHD flow and heat transfer over a vertical stretching plate embedded in a non-Darcian porous medium in the presence of rapid heating/cooling. By using similarity approach, the transport equations are transformed into non-linear ordinary differential equations and they are solved by Runge-Kutta-Fehlberg method along with shooting technique. From the present study the following conclusions may be drawn:

- An increase in the unsteady parameter is to decrease the thickness of the momentum boundary layer for all the governing parameters.
- The velocity profile decreases with an increase in the values of magnetic parameter $M$, whereas reverse trend is seen with increase in the buoyancy parameter $\lambda$.
- By applying non-Darcy effects in the flow field, the fluid velocity is decreased, but the reverse behaviour is seen in the temperature field for fluid and solid-matrix phases.
- During the process of rapid heating, the Sparrow-Gregg-type "hill" is appeared in the temperature profile for solid-matrix and fluid phases. Meanwhile, it is controlled by transient parameter $A$.
- For all the cases of $Pr$, $Q$ and $A$, the larger temperature difference between the fluid-solid phases is observed in the region of lower values of $H$ or $\gamma$. Once again it is concluded that the larger values of $H$ or $\gamma$ correspond to attain thermal equilibrium (LTE) between the phases.
- When $H$ or $\gamma$ increases, heat sink parameters lead to attain thermal equilibrium quickly. But the heat source parameters delayed it.
- The rate of heat transfer for fluid and solid phases increases with an increase in the Prandtl number and transient parameter, but the reverse effect has been observed in the enhancement of heat generation/absorption parameters.

## References

[1] K. VAJRAVELU, *Flow and heat transfer in a saturated porous medium over a stretching surface*, Z. Angew. Math. Mech., 74 (1994), pp. 605–614.
[2] D. A. NIELD AND A. BEJAN, Convection in Porous Media, Springer, New York, 2013.
[3] K. VAFAI, Handbook of Porous Media, Taylor & Francis, New York, 2005.
[4] D. B. INGHAM AND I. POP, Transport Phenomena in Porous Media, Vol. III. Elsevier, Oxford, 2005.
[5] K. VAFAI AND C. L. TIEN, *Boundary and inertia effects on flow and heat transfer in porous media*, Int. J. Heat Mass Transfer, 24 (1981), pp. 195–203.
[6] C. H. CHEN AND C. K. CHEN, *Non-Darcian mixed convection along a vertical plate embedded in a porous medium*, Appl. Math. Model., 14 (1990), pp. 482–488.

[7] E. M. A. ELBASHBESHY AND M. A. A. BAZID, *The mixed convection along a vertical plate with variable surface heat flux embedded in porous medium*, Appl. Math. Comput., 125 (2002), pp. 317–324.
[8] C. Y. CHENG, *Non-Darcy natural convection heat and mass transfer from a vertical wavy surface in saturated porous media*, Appl. Math. Comput., 182 (2006), pp. 1488–1500.
[9] I. A. HASSANIEN AND T. H. AL-ARABI, *Non-Darcy unsteady mixed convection flow near the stagnation point on a heated vertical surface embedded in a porous medium with thermal radiation and variable viscosity*, Commun. Nonlinear Sci. Numer. Simulat., 14 (2009), pp. 1366–1376.
[10] H. ROSALI, A. ISHAK AND I. POP, *Mixed convection stagnation-point flow over a vertical plate with prescribed heat flux embedded in a porous medium: brinkman-extended darcy formulation*, Transp Porous Med., 90 (2011), pp. 709–719.
[11] D. PRAKASH, M. MUTHTAMILSELVAN AND DEOG-HEE DOH, *Unsteady MHD non-Darcian flow over a vertical stretching plate embedded in a porous medium with non-uniform heat generation*, Appl. Math. Comput., 236 (2014), pp. 480–492.
[12] M. KAVIANY, Principles of Heat Transfer in Porous Media, Second ed., Springer, New York, 1999.
[13] N. SANJUAN, S. SIMAL, J. BON AND A. MULET, *Modelling of broccoli stems rehydration process*, J. Food Eng., 42 (1999), pp. 27–31.
[14] S. E. ZORRILLA AND A. C. RUBIOLO, *Mathematical modeling for immersion chilling and freezing of foods. Part I. Model development*, J. Food. Eng., 66 (2005), pp. 329–338.
[15] D. D. DINCOV, K. A. PARROTT AND K. A. PERICLEOUS, *Heat and mass transfer in two-phase porous materials under intensive microwave heating*, J. Food Eng., 65 (2004), pp. 403–412.
[16] V. V. CALMIDI AND R. L. MAHAJAN, *Forced convection in high porosity foams*, ASME J. Heat Transfer, 122 (2000), pp. 557–565.
[17] C. Y. ZHAO, T. J. LU AND H. P. HODSON, *Thermal radiation in ultralight metal foams with open cells*, Int. J. Heat Mass Transfer, 47 (2004), pp. 2927–2939.
[18] N. H. SAEID, *Analysis of free convection about a horizontal cylinder in a porous media using a thermal non-equilibrium model*, Int. Commun. Heat Mass Transfer, 33 (2006), pp. 158–165.
[19] A. C. BAYTAS AND I. POP, *Free convection in a square porous cavity using a thermal nonequilibrium model*, Int. J. Thermal. Sci., 41 (2002), pp. 861–870.
[20] A. C. BAYTAS, *Thermal non-equilibrium natural convection in a square enclosure filled with a heat-generating solid phase, non-Darcy porous medium*, Int. J. Energy Res., 27 (2003), pp. 975–988.
[21] A. N. BORUJERDI, A. R. NOGHREHABADI AND D. A. S. REES, *Onset of convection in a horizontal porous channel with uniform heat generation using a thermal nonequilibrium model*, Transport Porous Media, 69 (2007), pp. 343–357.
[22] K. C. WONG AND N. H. SAEID, *Numerical study of mixed convection on jet impingement cooling in a horizontal porous layer under local thermal non-equilibrium conditions*, Int. J. Thermal Sci., 48 (2009), pp. 860–870.
[23] D. A. S. REES AND I. POP, *Vertical free convection boundary layer flow in a porous medium using a thermal non-equilibrium model*, J. Porous Media, 3 (2001), pp. 31–44.
[24] N. H. SAEID, *Analysis of mixed convection in a vertical porous layer using non-equilibrium model*, Int. J. Heat Mass Transfer, 47 (2004), pp. 5619–5627.
[25] A. NOURI-BORUJERDI, A. R. NOGHREHABADI AND D. A. S. REES, *The effect of local thermal non-equilibrium on conduction in porous channels with a uniform heat source*, Transp Porous Med., 69 (2007), pp. 281–288.
[26] M. NAZARI AND F. KOWSARY, *Analytical solution of non-equilibrium heat conduction in porous medium in-corporating a variable porosity model with heat generation*, J. Heat Transfer, 131 (2009),

014503.

[27] A. BARLETTA AND M. CELLI, *Local thermal non-equilibrium flow with viscous dissipation in a plane horizontal porous layer*, Int. J. Thermal. Sci., 50 (2011), pp. 53–60.

[28] M. MUTHTAMILSELVAN, D. PRAKASH AND DEOG-HEE DOH, *Effect of thermal non-equilibrium on transient hydromagnetic flow over a moving surface in a nanofluid saturated porous media*, J. Mech. Sci. Tech., 28 (2014), pp. 3709–3718.

[29] N. H. SAEID AND A. A. MOHAMAD, *Periodic free convection from a vertical plate in a saturated porous medium-Non-equilibrium model*, Int. J. Heat Mass Transfer, 48 (2005), pp. 3855–3863.

[30] M. S. MALASHETTY, I. POP AND R. HEERA, *Linear and nonlinear double diffusive convection in a rotating sparsely packed porous layer using a thermal non-equilibrium model*, Continuum. Mech. Thermodyn., 21 (2009), pp. 317–339.

[31] A. ISHAK, R. NAZAR AND I. POP, *Heat transfer over an unsteady stretching permeable surface with prescribed wall temperature*, Nonlinear Anal. Real World Appl., 10 (2009), pp. 2909–2913.

[32] M. MUTHTAMILSELVAN AND D. PRAKASH, *Unsteady hydromagnetic slip flow and heat transfer of nanofluid over a moving surface with prescribed heat and mass fluxes*, Proc. I Mech. E Part C J. Mech. Eng. Sci., 229 (2015), pp. 703–715.

[33] A. PANTOKRATORAS, *A common error made in investigation of boundary layer flows*, Appl. Mathemat. Model., 33 (2009), pp. 413–422.

[34] A. ISHAK, R. NAZAR AND I. POP, *Boundary layer flow and heat transfer over an unsteady stretching vertical surface*, Meccanica, 44 (2009), pp. 369–375.

[35] K. VAJRAVELU, K. V. PRASAD AND NG. CHIU-ON, *Unsteady convective boundary layer flow of a viscous fluid at a vertical surface with variable fluid properties*, Nonlinear Anal. Real World Appl., 14 (2013), pp. 455–464.